The Journal of Immunology

Anti-Inflammatory and Proresolving Effects of the Omega-6 Polyunsaturated Fatty Acid Adrenic Acid

Hilde Brouwers, Hulda S. Jónasdóttir, Marije E. Kuipers, Joanneke C. Kwekkeboom, Jennifer L. Auger, Mayra Gonzalez-Torres, Cristina López-Vicario, Joan Clària, Jona Freysdottir, Ingibjorg Hardardottir, José Garrido-Mesa, Lucy V. Norling, Mauro Perretti, Tom W. J. Huizinga, Margreet Kloppenburg, René E. M. Toes, Bryce Binstadt, Martin Giera and Andreea Ioan-Facsinay

J Immunol published online 2 October 2020
http://www.jimmunol.org/content/early/2020/10/01/jimmunol.1801653

Supplementary Material **http://www.jimmunol.org/content/suppl/2020/10/01/jimmunol.1801653.DCSupplemental**

The Journal of Immunology is published twice each month by
The American Association of Immunologists, Inc.,
1451 Rockville Pike, Suite 650, Rockville, MD 20852

Print ISSN: 0022-1767 Online ISSN: 1550-6606.

Published October 2, 2020, doi:10.4049/jimmunol.1801653

Anti-Inflammatory and Proresolving Effects of the Omega-6 Polyunsaturated Fatty Acid Adrenic Acid

Hilde Brouwers,* Hulda S. Jónasdóttir,*,† Marije E. Kuipers,† Joanneke C. Kwekkeboom,* Jennifer L. Auger,‡,§ Mayra Gonzalez-Torres,‡,§ Cristina López-Vicario,¶ Joan Clària,¶ Jona Freysdottir,‖ Ingibjorg Hardardottir,‖ José Garrido-Mesa,# Lucy V. Norling,# Mauro Perretti,# Tom W. J. Huizinga,* Margreet Kloppenburg,* René E. M. Toes,* Bryce Binstadt,‡,§ Martin Giera,†,1 and Andreea Ioan-Facsinay*,1

Polyunsaturated fatty acids (PUFAs) and their metabolites are potent regulators of inflammation. Generally, omega (*n*)-3 PUFAs are considered proresolving whereas *n*-6 PUFAs are classified as proinflammatory. In this study, we characterized the inflammatory response in murine peritonitis and unexpectedly found the accumulation of adrenic acid (AdA), a poorly studied *n*-6 PUFA. Functional studies revealed that AdA potently inhibited the formation of the chemoattractant leukotriene B_4 (LTB_4), specifically in human neutrophils, and this correlated with a reduction of its precursor arachidonic acid (AA) in free form. AdA exposure in human monocyte-derived macrophages enhanced efferocytosis of apoptotic human neutrophils. In vivo, AdA treatment significantly alleviated arthritis in an LTB_4-dependent murine arthritis model. Our findings are, to our knowledge, the first to indicate that the *n*-6 fatty acid AdA effectively blocks production of LTB_4 by neutrophils and could play a role in resolution of inflammation in vivo. ***The Journal of Immunology*****, 2020, 205: 000–000.**

Inflammation is an important first-line response to barrier breach and tissue damage. Usually, inflammation and its resolution are tightly controlled processes that involve the recruitment of immune cells and soluble mediators. Lack of proper resolution can lead to chronic inflammation, which is associated with several diseases such as atherosclerosis, autoimmune diseases, asthma, and cancer. During the past 20 y, it has been established that polyunsaturated fatty acids (PUFAs) and PUFA-derived lipid mediators are potent regulators of inflammation and its resolution (1).

Historically, *n*-6 PUFAs such as arachidonic acid (AA) and linoleic acid (LA) are considered proinflammatory, whereas *n*-3 PUFAs are considered to be anti-inflammatory and/or proresolving (2). This is primarily because of the fact that the potent proinflammatory leukotrienes and PGs are derived from AA. In contrast, *n*-3 PUFAs such as eicosapentaenoic acid (EPA), docosahexaenoic acid (DHA), and docosapentaenoic acid (DPA) are metabolized into so-called specialized proresolving lipid mediators (SPMs) like resolvins, protectins and maresins (1, 3–5). In addition to SPMs derived from EPA, DHA and DPA, more recently, additional *n*-3-PUFA–derived metabolites have been associated with anti-inflammatory effects, such as the 15-lipoxygenase (LOX) products from α-LA (6). Furthermore, biological functions have been assigned to the free *n*-3 PUFAs themselves (7). For instance, EPA, DHA, and DPA can compete with AA as substrates for enzyme conversion, leading to a diminished production of proinflammatory oxylipins (8). Moreover, free *n*-3 PUFAs can mediate anti-inflammatory effects by activating their specific G protein–coupled receptor GPR120 (9).

However, this pro- versus anti-inflammatory classification of *n*-6 and *n*-3 PUFAs might be too strict. On the molecular level, anti-inflammatory effects of *n*-6 PUFAs and their derivatives have been shown both in vitro and in vivo. For instance, AA can be metabolized into proresolving lipoxins as well as anti-inflammatory cytochrome P450 (Cyp450) derivatives (10, 11). Furthermore, AA-derived PG E_2 (PGE_2) was shown to have both proinflammatory and proresolution properties (12). In addition, earlier studies proposed that the *n*-6 PUFAs dihomo-γ-linolenic acid (DGLA) and adrenic acid (AdA) might compete with AA for proinflammatory oxylipin production (13–18).

Clinical trials using *n*-3 PUFA supplementation in several inflammatory diseases have shown both beneficial but also negative results. Systematic reviews in asthma and rheumatoid arthritis

*Department of Rheumatology, Leiden University Medical Center, 2333 ZA Leiden, the Netherlands; †Center for Proteomics and Metabolomics, Leiden University Medical Center, 2333 ZA Leiden, the Netherlands; ‡Department of Pediatrics and Center for Immunology, University of Minnesota Medical School, Minneapolis, MN 55454; §Center for Immunology, University of Minnesota Medical School, Minneapolis, MN 55455; ¶Hospital Clínic-IDIBAPS, University of Barcelona, 08007 Barcelona, Spain; ‖University of Iceland and Landspitali—The National University Hospital of Iceland, 101 Reykjavik, Iceland; and #William Harvey Research Institute, Barts and the London School of Medicine, Queen Mary University of London, London E1 4NS, United Kingdom

[1]M.G. and A.I.-F. contributed equally.

ORCIDs: 0000-0001-7012-3004 (M.E.K.); 0000-0003-4333-7749 (J.C.); 0000-0001-9461-182X (J.F.); 0000-0003-0178-7047 (I.H.); 0000-0001-6420-9055 (J.G.-M.); 0000-0001-5316-9115 (L.V.N.); 0000-0003-2068-3331 (M.P.); 0000-0002-9618-6414 (R.E.M.T.); 0000-0003-3127-3856 (B.B.); 0000-0003-1684-1894 (M.G.).

Received for publication January 28, 2019. Accepted for publication September 7, 2020.

Address correspondence and reprint requests to Dr. Martin Giera, Leiden University Medical Center, Center for Proteomics and Metabolomics, Zone P1-Q, Albinusdreef 2, 2333 ZA Leiden, the Netherlands. E-mail address: m.a.giera@lumc.nl

The online version of this article contains supplemental material.

Abbreviations used in this article: AA, arachidonic acid; AdA, adrenic acid; $cPLA_2$, cytosolic phospholipase A2; DAG, diacylglyceride; DHA, docosahexaenoic acid; DMS, differential mobility separation; DPA, docosapentaenoic acid; EPA, eicosatetraenoic acid; EtOH, ethanol; GC-MS, gas chromatography–mass spectrometry; G6PI, glucose-6-phosphate isomerase; IS, internal standard; LA, linoleic acid; LC-MS/MS, liquid chromatography–tandem mass spectrometry; LTB_4, leukotriene B_4; LUMC, Leiden University Medical Center; MeOH, methanol; PC, phosphatidylcholine; PUFA, polyunsaturated fatty acid; SPM, specialized proresolving lipid mediator; TAG, triglyceride.

report inconsistent or modest beneficial effects and also in cardiovascular disease, *n*-3 PUFA supplementation trials did not show conclusive beneficial effects (19–23). Furthermore, some studies report beneficial effects of dietary *n*-6 PUFA intake, in particular with regard to LA (24, 25). In summary, several reports highlight that a simple dichotomous classification of *n*-6 and *n*-3 PUFA as exclusively pro- and anti-inflammatory, respectively, does not sufficiently describe the underlying biology and that the pro- and anti-inflammatory roles of PUFAs are not completely understood.

To better understand the roles of the *n*-3 and *n*-6 PUFA in the context of inflammation, we determined their kinetics in an experimental model of self-resolving peritonitis. We performed a comprehensive analysis of lipids, using liquid chromatography–tandem mass spectrometry (LC-MS/MS) and we discovered the accumulation of the *n*-6 PUFA AdA during the resolution phase of inflammation. This finding triggered us to further study the biological function of AdA in vitro and in vivo.

Materials and Methods

Cell isolation and culture

Human primary neutrophils were isolated from EDTA blood of healthy donors. Most of the erythrocytes were removed by dextran sedimentation using 3% dextran T-500 (Pharmacosmos) in PBS without calcium and magnesium [PBS ($^{-/-}$); Lonza]. Next, neutrophils were separated from PBMCs by Ficoll density gradient centrifugation and remaining erythrocytes were removed by hypotonic lysis. Human PBMCs were isolated from buffy coats of healthy donors (Sanquin, Amsterdam, the Netherlands) by Ficoll density gradient centrifugation. Monocytes were isolated from PBMCs by magnetic cell sorting using $CD14^+$ microbeads (Miltenyi Biotec) and were differentiated in RPMI 1640 (Life Technologies) supplemented with 8% FCS using 5 ng/ml GM-CSF (R&D Systems) for 7 d. Written informed consent was obtained from all donors and the study was approved by the medical ethical committee of the Leiden University Medical Center (LUMC).

Cell culture incubations for lipid analysis

Neutrophils (1×10^6 cells/ml) were incubated with 5 μg/ml AdA (Nu-Check Prep) in PBS with calcium and magnesium [($^{+/+}$); B. Braun] for 10 min. Macrophages were incubated for either 10 min or 24 h, using the same cell density and AdA concentration as for neutrophils, but in RPMI 1640 without phenol red (Life Technologies) containing 0.1% fatty acid–free BSA (Sigma-Aldrich). AdA was prediluted in ethanol (EtOH, absolute HPLC grade; Thermo Fisher Scientific) and suspended in the appropriate medium using an ultrasonic bath. After stimulation with AdA, both neutrophils and macrophages were stimulated with 4 μM calcium ionophore A23187 (Sigma-Aldrich) for 10 min. For lipid mediator analysis, methanol (MeOH) containing internal standards (IS) was added to the cells and their supernatant in a 3:1 volume ratio. The IS consisted of leukotriene B_4 (LTB_4)–d4, PGE_2-d4, 15-HETE-d8 (all 50 ng/ml), and 500 ng/ml of DHA-d5. Samples were stored under argon at −80˚C until analysis. For quantitative lipidomic analysis using the Lipidyzer, the cells were washed twice with PBS ($^{+/+}$) containing 0.1% fatty acid–free BSA after stimulation. The pelleted cells were stored at −80˚C until analysis.

Calcium flux assay

Leukocytes were obtained from heparinized blood of healthy donors. To this end, HetaSep (Stemcell Technologies) was added to the blood at a ratio of 1:6 (HetaSep: blood) and incubated for 30 min at 37˚C to sediment the erythrocytes. Leukocytes were harvested and remaining erythrocytes were lysed using NH4Cl/KHCO3 (5 min, room temperature). Leukocytes (1×10^7/ml) in RPMI 1640 containing 2% FCS and 0.02% pluronic acid (Molecular Probes) were labeled with 2 μM Indo-1 AM (Molecular Probes) for 35 min at 37˚C. Cells were washed and resuspended in RPMI 1640 containing 2% FCS and 1 mM CaCl2. Cells were preincubated (10 min, 37˚C) with 5 μg/ml AdA before acquisition. After 2 min of acquisition, calcium ionophore A23187 was added and samples were acquired another 5 min. Cells were analyzed by flow cytometry using an LSRII (BD Biosciences) and analyzed using FlowJo software.

Phagocytosis assay

THP-1 cells were differentiated in the presence of PMA (50 ng/ml) for 48 h, followed by medium exchange to RPMI 1640 supplemented with 10% FCS for 24 h. Differentiated THP-1 cells (96-well plate, 35,000 cells per well) were pretreated with AdA or vehicle (15 min, 37˚C), followed by the addition of opsonized FITC-labeled zymosan A (Molecular Probes) at a ratio of 10:1 (particles/cell) for 1 h at 37˚C. FITC-labeled zymosan A was opsonized using opsonizing reagent containing purified rabbit polyclonal IgG Abs (Molecular Probes, Eugene, OR). Subsequently, trypan blue solution (0.04%; Sigma-Aldrich) was used to quench surface-bound FITC-zymosan A particles for 2 min at room temperature after which the solution was washed away and substituted with PBS ($^{+/+}$). Fluorescence intensity was measured in a FluoStar Optima Microplate Reader (BMG Labtech) using an excitation of 485 nm and an emission of 520 nm.

Efferocytosis assay

PBMCs were isolated by density centrifugation of leukocyte cones from the National Health Service Blood and Transplant Bank. PBMCs were plated 30×10^6 cells per 10 cm^2 in PBS ($^{+/+}$). After 1 h, the cells were washed twice, after which monocytes remained adhered to the plate. The monocytes were differentiated in RPMI 1640 (Sigma-Aldrich) supplemented with 20% FBS in the presence of 50 ng/ml hM-CSF (PeproTech) for 7 d. Macrophages (M0 macrophages) were harvested and plated (96-well plate, 2.5×10^4 cells per well) and polarized to become M1 macrophages under the influence of IFN-γ (20 ng/ml; PeproTech) and LPS (10 ng/ml; Sigma-Aldrich) for 24 h. Apoptotic HL-60 cells were prepared by incubating the cells in serum free PBS for 24 h (4×10^6 cells/ml) after which ∼60% is apoptotic. Apoptotic HL-60 cells were labeled with CFSE (2 μM, 37˚C, 10 min). M0 and M1 macrophages were pretreated with AdA (Cayman Chemicals) for 30 min at 37˚C. Apoptotic HL-60 cells were added in a 1:5 ratio (macrophages/HL-60 cells) and left to incubate for 1 h at 37˚C. Subsequently, macrophages were washed twice, and surface-bound HL60 were quenched with trypan blue solution (0.04%; Sigma-Aldrich) for 2 min at room temperature. CFSE-positive efferocytic macrophages were detected using an LSR Fortessa II and data were analyzed using FlowJo software.

Migration assay

Isolated human neutrophils (1×10^6 cells/ml) were incubated with 5 μg/ml AdA in PBS ($^{+/+}$) or vehicle (1% EtOH) for 10 min and subsequently stimulated with 4 μM calcium ionophore A23187 for 10 min. Next, the cells were centrifuged (16,100 × *g*, 10 min), and supernatant was stored at −80˚C until further use. For the migration assay, 29 μl of supernatant was added to the bottom well of a ChemoTx plate (101-3; Neuro Probe) and 25 μl containing 2×10^5 freshly isolated neutrophils was added to the upper well. Migrated cells were collected from the lower well after 90 min at 37˚C. The cells were quantified by flow cytometry using an LSRFortessa (BD Biosciences), Flow-Count Fluorospheres (Beckman Coulter), and FACSDiva software (BD Biosciences).

Enzyme activity assays

Activity assays were performed according to the manufacturers' protocol. The Lipase Activity Assay Kit (Sigma-Aldrich) and the $cPLA_2$ Assay Kit (Cayman Chemicals) were used.

In vivo peritonitis model

This experiment was both carried out at the University of Iceland and at the LUMC. Male C57BL/6 mice of 8-wk-old were purchased from Charles River. Animals were housed in the local animal facility in individually ventilated cages. Peritonitis was induced by injecting 1 mg of zymosan A (*Saccharomyces cerevisiae*; Sigma-Aldrich) in 100 μl of saline i.p. Control mice were injected with saline only. AdA-treated mice were injected with 10 μg AdA in saline either at timepoint $t = 0$ or $t = 2$ h. In the experiments in which mice were treated with AdA at $t = 0$, AdA was mixed with the zymosan A to limit the number of injections. AdA was prediluted in absolute HPLC–grade EtOH and EtOH was evaporated using a SpeedVac (Zirbus). Next, AdA was suspended in saline using an ultrasonic bath. Saline for control mice was treated identically, without the addition of AdA. Control and AdA-treated mice were randomized over the cages and were housed together in a cage. At the indicated time points after induction of peritonitis, mice were sacrificed by exposure to carbon dioxide and peritoneal lavage was collected using 5 ml of ice-cold PBS. From this lavage, cells were collected by centrifugation (10 min, 225 × *g*). Part of the recruited cells were analyzed by flow cytometry using anti-F4/80 (BM8; BioLegend) and anti-GR1 (1A8; BD Biosciences), or anti-CD11b (M1/70; BD Bioscience) and anti-CXCR2 (TG11; BioLegend). Cells were counted by light microscopy and were analyzed using Navios Flow Cytometer and Kaluza software (Beckman Coulter). For lipid mediator analysis, the remaining peritoneal cells were centrifuged at 16,100 × *g* for

5 min and snap frozen. The pelleted cells were stored at −80°C until use. On the day of analysis, 250 μl of EtOH was added to the cells, samples were shaken for 5 min, ultrasonicated for 10 s and centrifuged at 16,100 × *g* for 5 min. The remaining pellet was used to measure protein content using Pierce BCA Protein Assay Kit (Thermo Fisher Scientific). Peritoneal lavage samples were worked up using solid-phase extraction as published previously (26) without the *n*-hexane–washing step, as free fatty acids were to be evaluated, and resuspended in a final volume of 200 μl of 40% MeOH. The study was approved by the Experimental Animal Committee, Ministry for the Environment in Iceland, and the Ethical Committee for Animal Experimentation of the LUMC.

K/BxN serum–transferred arthritis and anti-G6PI ELISA

These experiments were both carried out at the University of Minnesota Medical School and the LUMC. Male C57BL/6 mice of 8-wk-old were purchased from Charles River or The Jackson Laboratory. Animals were housed in the local animal facility in individually ventilated cages. Mice on different treatments were kept in separate cages. Arthritis was induced by i.p. injection of 100 μl of arthritic serum, obtained from TCR-transgenic K/BxN mice; injections were done on day 0 and day 2. Mice were treated daily with 2.5 mg AdA from day −3 to the end of the experiment. AdA was dissolved fresh each day in Cremophor EL (Calbiochem) in a 1:1 ratio before dissolving in saline, resulting in a 2.5% final concentration Cremophor. Control mice were treated with 2.5% Cremophor in saline. Clinical scores were obtained in a blinded fashion as previously described (27). In short, a clinical score of 0–3 was given to each paw daily. In addition, ankle thickness of both left and right ankle was measured daily using a precision caliper. Ankle difference was calculated by combining the score of the left and right ankle daily and subtracting the combined baseline thickness, divided by two. Anti–glucose-6-phosphate isomerase (anti-G6PI) Abs were measured in plasma taken at day 10 and day 14 via a tail vein bleed, or in serum obtained at the end of the experiment via heart puncture. The study was approved by the Institutional Animal Care and Use Committee in the United States and the Ethical Committee for Experimental Animal Experimentation of the LUMC, depending on where the experiments were carried out. Anti-G6PI Abs were analyzed as described before (28). AdA was diluted in serum of either arthritic or nonarthritic mice or PBS, resulting in different AdA concentrations to test interference with the detection of anti-G6PI Abs by ELISA.

Chemicals

5-HETE, 5*S*-HETE, 8-HETE, 11-HETE, 12-HETE, 15-HETE, 15-HEPE, 18-HEPE, 17R-HDHA, 14,15-diHETE, 7S,17S-diHDPA, LXA_4, AT-LXA_4, LXB_4, LTB_4, 6-*trans*, 12-epi-LTB_4, 6-*trans*-LTB_4, 20-OH-LTB_4, PGD_2, PGE_2, $PGF_{2\alpha}$, TXB_2, RvD1, RvD2, 10*S*,17*S*-diHDHA, MaR1, LTD_4, LTE_4, 19,20-diHDPA, 8*S*,15*S*-diHETE, DPAn-3, DHA, and EPA were from Cayman Chemicals and used to construct calibration lines. 15*S*-HETE-d8, LTB_4-d4, PGE_2-d4, and DHA-d5 were used as IS (Cayman Chemicals). RvE1, RvE2, synthetic 18*S*-RvE3, and 18*R*-RvE3 were kind gifts from Dr. M. Arita (RIKEN, Yokohama, Japan). AdA and the GLC-85 standard mix were from Nu-Check Prep. All other chemicals, including Fluka LC-MS CHROMASOLV–grade MeOH, were from Sigma-Aldrich.

Lipidomic analyses

LC-MS/MS analysis was carried out as previously described (26) on a QTrap 6500 mass spectrometer (Sciex), coupled to a Shimadzu Nexera LC30-system including autosampler and column oven (Shimadzu). The employed column was a Kinetex C18 50 × 2.1 mm, 1.7 μm, protected with a C8 precolumn (Phenomenex). Water (A) and MeOH (B), both with 0.01% acetic acid, were used. The gradient program started at 40% eluent B and was kept constant for 1 min, then linearly increased to 45% B at 1.1 min, then to 53.5% B at 4 min, to 55% B at 6.5 min, then to 90% B at 12 min and finally to 100% B at 12.1 min, kept constant for 3 min. The flow rate was set to 400 μl/min. The mass spectrometer was operated under the following conditions: the collision gas flow was set to medium, the drying temperature was 400°C, the needle voltage was −4500 V, the curtain gas was 30 ψ, ion source gas 1 was 40 ψ, and the ion source gas 2 was 30 ψ (air was used as drying gas and nitrogen as curtain gas). LC-MS/MS peaks were integrated with manual supervision and area corrected to corresponding IS using MultiQuant 2.1 (Sciex). For quantification, the multiple-reaction monitoring transitions and collision energies were used, combined with calibration lines.

For gas chromatography–mass spectrometry (GC-MS) analysis, to 1 × 10^6 neutrophils or macrophages were added 250 μl of acetone (HPLC grade; Sigma-Aldrich) in 20 μl of PBS ($^{-/-}$) and 10 μl of EtOH (Merck). Next, lipids were hydrolyzed using 10 μl of 10 mM sodium hydroxide for 30 min at 60°C. After hydrolysis, 1 μl/ml IS was added and sample workup and PUFA quantification was performed as previously described (29). GC-MS was performed using a Scion 436 gas chromatograph coupled to a Scion triple quadrupole mass spectrometer (both from Bruker) including a G6501-CTC PAL autosampler (CTC analytics).

For Lipidyzer analysis, 250 μl of 2-propanol was added to 5 × 10^6 neutrophils and centrifuged for 10 min at 16,000 × *g* at 20°C. Supernatant was collected and the pellet was subjected to additional extraction using 200 μl of 2-propanol. One hundred microliters of IS in MeOH/dichloromethane was added and the sample was dried under a gentle stream of nitrogen. The sample was suspended in 250 μl of 10 mM ammonium acetate in (50:50) MeOH/dichloromethane. Acquisition and quantification was performed as previously described using a QTrap 5500 mass spectrometer (Sciex) with differential mobility separation (DMS) coupled to a Shimadzu Nexera ×2 LC System for flow injection and Lipidomics Workflow Manager Software (30, 31).

Statistical analysis

Significance was calculated by means of two-tailed unpaired Student *t* tests, one-way or two-way ANOVA, or a two-tailed Wilcoxon signed-rank test for paired samples using GraphPad Prism version 7.04 for Windows. To justify using two-way ANOVA in Figs. 5 and 6 and Supplemental Fig. 3, the Shapiro–Wilk test was used. To determine statistical significance by linear-mixed model analysis or repeated measures ANOVA as a mixed model, IBM SPSS Statistics 25 for Windows was used. The statistical test used to determine significance is indicated for each experiment.

Results

Cellular accumulation of AdA during resolution

First, we carried out a detailed molecular mapping of the self-resolving zymosan A-induced murine peritonitis model. Using a validated LC-MS/MS platform, we analyzed the cellular PUFA and oxylipin content in a longitudinal fashion (Fig. 1A). It was previously shown in this model that PUFAs, as well monohydroxylated fatty acids, leukotrienes, and PGs, accumulate in the cell-free lavage fluid during the peak of inflammation and their levels return to baseline during resolution (29, 30). We confirmed this accumulation of PUFAs in the cell-free lavage in our first experiment (Supplemental Fig. 1A). Moreover, we show that inside the cells, the kinetics are different: the monohydroxylated products accumulate only during the resolution phase, which was characterized by the decrease of neutrophil numbers and the increase of $F4/80^+$ expression on macrophages (Supplemental Fig. 1B, 1C) (31). Leukotriene B_4 (LTB_4) levels peak at 12 h after which levels again decrease, in contrast to the PGs, which show a biphasic pattern. The analysis revealed a particular accumulation of free PUFAs in the cellular fraction during the resolution phase of inflammation (Fig. 1A). The PUFA accumulation varied largely between different PUFAs: levels of free LA and α-LA changed only marginally (between 3- and 5-fold) compared with baseline, whereas DHA levels increased the most (133-fold). Furthermore, we detected a strong increase of 80-fold for the *n*-6 fatty acid AdA within the cellular fraction (Fig. 1B), suggesting a previously unappreciated proresolving role for this *n*-6 PUFA. This increase was observed in three independent experiments of which two were performed at the University of Iceland and one at the LUMC in the Netherlands (Fig. 1C). To test the proresolving capacity of AdA, we administered AdA either simultaneously with zymosan or 2 h after peritonitis induction. In both experiments, we detected an enhanced neutrophil clearance from the peritoneal cavity (Fig. 1D, 1E). These results prompted us to further investigate the role of AdA in inflammatory responses.

AdA inhibits LTB_4 production in neutrophils

We initially investigated the effect of AdA on the oxylipin and PUFA profile of human primary neutrophils and macrophages, as these are key players in acute inflammation in humans as well as the main cell populations present in the peritoneal cavity during the first 72 h of inflammation (29, 32). Our analysis revealed that AdA

A

Analyte	Time (hours) 0	2	4	12	24	48	72
5-HETE	0,1	0,7	3,2	3,9	3,2	2,5	10,6
8-HETE	0,3	0,5	0,4	0,3	0,2	0,6	2,6
11-HETE	1,1	0,4	2,2	1,5	1,3	0,8	5,7
12-HETE	28,1	12,7	10,7	9,2	4,8	17,5	64,5
15-HETE	1,0	1,7	3,3	2,1	1,5	2,5	12,4
15-HEPE	0,1	0,5	0,8	0,5	0,4	1,9	2,5
18-HEPE	0,0	0,0	0,1	0,0	0,0	0,0	0,1
17-HDHA	0,7	2,6	6,0	2,3	1,5	12,6	32,5
LTB_4	0,0	0,1	2,1	2,4	1,6	0,0	0,0
6-trans-LTB_4	3,0	0,2	0,2	0,3	0,2	0,1	0,3
6-trans-12-epi-LTB_4	4,0	0,2	0,2	0,2	0,2	0,1	0,5
20-OH-LTB_4	0,0	0,0	0,0	0,0	0,0	0,0	0,0
LTD_4	0,0	0,2	0,1	0,0	0,2	0,0	0,4
LTE_4	0,1	0,4	0,2	0,0	0,4	0,4	2,4
PGD_2	0,1	0,1	0,5	0,8	0,4	0,3	0,7
PGE_2	0,8	0,1	6,4	7,3	4,1	3,9	31,8
$PGF_{2\alpha}$	0,5	0,3	5,1	3,0	1,7	0,5	2,2
8-iso-PGE_2	0,0	0,0	0,1	0,1	0,1	0,1	0,7
8-iso-$PGF_{2\alpha}$	0,1	0,0	0,4	0,2	0,1	0,0	0,2
15-keto-PGE_2	0,1	0,0	0,0	0,0	0,0	0,0	0,0
LXA_4	0,0	0,0	0,0	0,0	0,0	0,0	0,0
AT-LXA_4	0,0	0,0	0,0	0,0	0,0	0,0	0,0
LXB_4	0,3	0,0	0,0	0,0	0,0	0,0	0,1
10S,17S-diHDHA	1,0	0,3	0,4	0,2	0,1	0,3	1,2
8S,15S-diHETE	0,9	0,1	0,1	0,1	0,0	0,1	0,4
7S,17S-diHDPA	0,1	0,0	0,0	0,0	0,0	0,0	0,1
14,15-diHETE	0,3	0,0	0,0	0,0	0,0	0,0	0,1
19,20-diHDPA	0,0	0,2	1,2	0,6	0,7	0,3	1,9
TXB_2	2,1	1,1	24,0	19,8	14,2	7,8	95,3
AA	22,7	93,6	279,6	479,1	690,7	488,2	1.037,9
EPA	1,5	4,7	13,3	31,0	49,5	36,7	22,9
DHA	2,1	18,2	106,8	134,2	194,0	156,6	287,3
AdA	2,0	9,5	25,2	52,4	76,2	69,7	164,8
DPA $_{n-3}$	11,6	13,8	44,7	81,5	125,6	127,4	182,3
ALA/GLA	16,8	20,1	44,3	58,3	91,2	65,4	61,2
LA	322,8	389,5	736,6	711,8	1.005,3	707,8	1.487,9

B

Analyte	Time (hours) 0	2	4	12	24	48	72
AA	1	4,1	12,3	21,1	30,4	21,5	45,6
EPA	1	3,2	9	21,1	33,6	24,9	15,5
DHA	1	8,5	49,7	62,4	90,3	72,9	133,7
AdA	1	4,6	12,3	25,6	37,3	34,1	80,6
DPA $_{n-3}$	1	1,2	3,8	7	10,8	11	14
ALA/GLA	1	1,2	2,6	3,5	5,4	3,9	3,6
LA	1	1,2	2,3	2,2	3,1	2,2	4,6

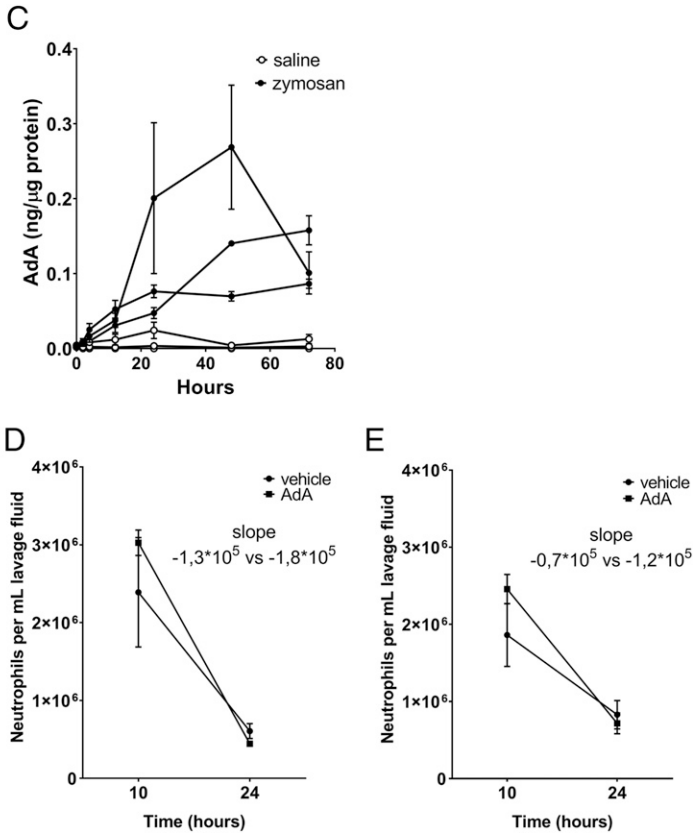

FIGURE 1. Time course of PUFA and their oxidative products during zymosan A-induced peritonitis. (**A**) Heat map of investigated lipids in the cellular fraction of peritoneal fluid (nanograms per milligram protein). $n = 3$ mice per time point; one representative experiment out of three is shown. (**B**) Fold change of detected PUFAs relative to the lowest detected concentration (timepoint zero) of the experiment as shown in (A). (**C**) Time course of free AdA accumulation in the cellular fraction of peritoneal fluid (nanograms per microgram protein) in three independent experiments depicted individually. Average with SEM of three to four mice per group is shown. (**D** and **E**) Mice were administered AdA at $t = 0$ h (D) or $t = 2$ h (E) and number of neutrophils in the peritoneal lavage was determined by flow cytometry. Mean and SEM are shown ($n = 5$–6 mice per group of two independent experiments).

diminished LTB_4 biosynthesis upon calcium ionophore A23187 stimulation in neutrophils, whereas there was an inconsistent effect on macrophages because of interdonor variations (Fig. 2A). In unstimulated cells the LTB_4 production pathway was not active (Supplemental Fig. 2A). Macrophages were incubated longer with AdA to reach similar AdA uptake, but experiments performed with 10 min incubation show similar results (data not shown). A similar effect was observed for the LTB_4 pathway marker 5-HETE (Fig. 2B). Besides LTB_4 and 5-HETE production, we could not detect any other eicosanoid formation such as PGs, nor could we detect any SPM formation within the experiment time frame. Because LTB_4 is produced upon AA release from phospholipids and triglycerides (33, 34) (Fig. 2C), we also measured the levels of released AA in AdA-treated cells (Fig. 2D). Interestingly, AA levels dramatically decreased upon AdA exposure in neutrophils, indicating that the entire LTB_4 production pathway is attenuated. In contrast, AdA led to an increase in AA in macrophages. Using three different cell viability assays we confirmed that the observed effect of AdA on neutrophil leukotriene synthesis was not caused by cell death (Supplemental Fig. 2B). In addition, we carried out intracellular calcium flux analysis showing that AdA-exposed neutrophils have an undisturbed intracellular calcium flux in response to calcium ionophore A23187 (Fig. 2E).

AdA-exposed neutrophils have reduced chemoattractant capacity

LTB_4 is a potent chemoattractant for neutrophils, so we next questioned if the downregulation of LTB_4 synthesis in neutrophils could have a functional effect. Indeed, LTB_4 and supernatant of calcium ionophore A23187–stimulated neutrophils attracted neutrophils in a *trans*-well system (Fig. 3B, Supplemental Fig. 2C). However, migration was strongly impaired when supernatant of stimulated AdA-exposed neutrophils was used (Fig. 3B). Any residual chemoattraction present is most likely due to incomplete inhibition of LTB_4 production (Fig. 3C) or to the presence of other chemoattractants that are released within 10 min of stimulation. Supernatant of unstimulated cells, AdA, or calcium ionophore A23187 alone were not able to induce neutrophil migration (Supplemental Fig. 2C).

AdA enhances macrophage phagocytosis

As macrophages play a crucial role in the resolution of inflammation, we next questioned whether AdA would also have an effect on macrophages. Several SPMs are able to enhance the phagocytic capacity of macrophages, a process involved in resolution of inflammation (1). We therefore examined whether AdA was able to enhance the phagocytosis of opsonized zymosan particles by THP-1–derived macrophages by 2.5-fold (Fig. 4A). In addition, we observed a 10.7- and 11.2-fold increase of efferocytosis of apoptotic HL-60 cells by monocyte-derived M0 and M1 macrophages, respectively (Fig. 4B).

AdA is internalized by neutrophils

We next set out to investigate the molecular mechanisms underlying the anti-inflammatory effects of AdA on neutrophils. Therefore, we studied whether AdA is taken up by the cells.

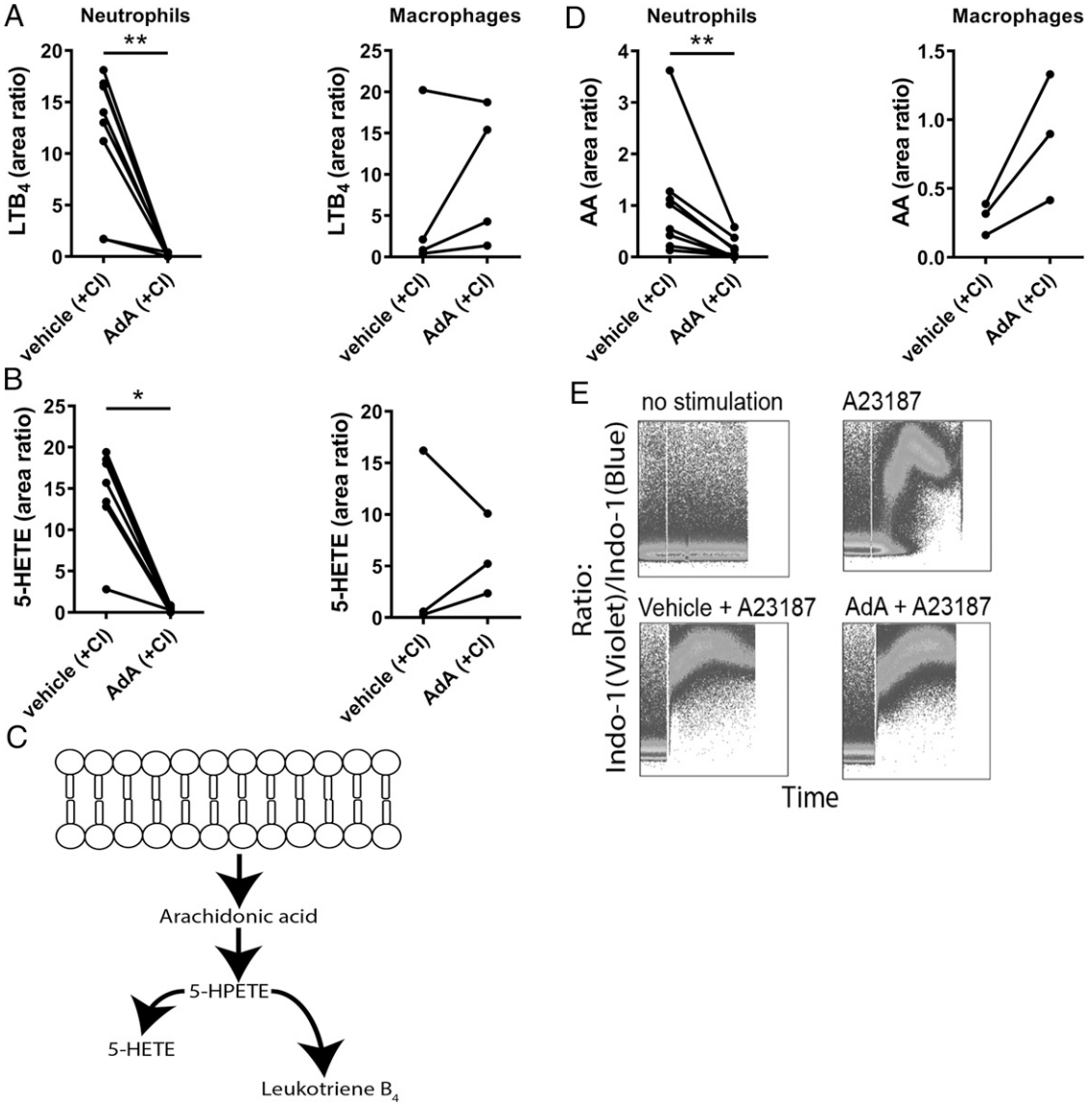

FIGURE 2. AdA inhibits LTB_4 production in neutrophils. (**A**, **B**, and **D**) Peripheral blood neutrophils and macrophages were preincubated for 10 min or 24 h with AdA, respectively, before stimulation with calcium ionophore A23187 for 10 min. Total free LTB_4, 5-HETE, and AA levels relative to IS were calculated based on LC-MS/MS signals (see *Materials and Methods*). Statistical significance was established using the Wilcoxon signed-rank test. Each line represents one donor (n = 3–8 donors, all individual experiments). (**C**) Schematic representation of the LTB_4 production pathway. (**E**) Calcium flux in peripheral blood neutrophils preincubated for 10 min with either vehicle or AdA and stimulated with calcium ionophore A23187. Experiment was performed once. $*p < 0.05$, $**p < 0.01$.

Using GC-MS based analysis, we showed increased total AdA levels in both neutrophils and macrophages upon 10 min and 24 h incubation with AdA, respectively, compared with vehicle (Fig. 5A, Supplemental Fig. 3A). Approximately 50% of the added 5 μg of AdA was found in the cellular fraction of both cell types after incubation. Next, we determined in which lipid reservoir AdA is stored to obtain an indication about the mechanisms underlying its inhibitory effect on AA release. To this end, we measured the neutrophil lipidome on a commercial lipidomics platform (Lipidyzer) and showed that AdA is stored in several different lipid reservoirs (Fig. 5B). We could not detect any AdA in lysophospholipids or sphingomyelin lipids in any of the conditions (data not shown). Instead AdA levels increased specifically in cholesteryl esters. AdA accumulation in phosphatidylcholines (PC), diacylglycerides (DAG), and triglycerides (TAG) was only detected after AdA incubation in combination with calcium ionophore A23187 stimulation. AdA did not accumulate in phosphatidylethanolamines (PE).

No apparent effects of AdA exposure on arrangement of AA in higher-order lipids

Because AdA accumulated in phospholipid species such as PC, as well as in DAG and TAG lipids, we hypothesized that AdA could affect the release of AA from these compartments. In addition to cytosolic phospholipase A2 ($cPLA_2$) it has been shown that adipose TAG lipase regulates AA release in neutrophils (34). We therefore investigated the activity of different lipases involved in AA release in these compartments. Surprisingly, AdA did not have an effect on either $cPLA_2$, measured by a phospholipase assay, or adipose TAG lipase activity, measured by a pan lipase assay (Fig. 6A). These enzymes release AA from phospholipids and TAGs, respectively. Because AdA does not appear to inhibit AA release by affecting lipase activity, we next sought to investigate in

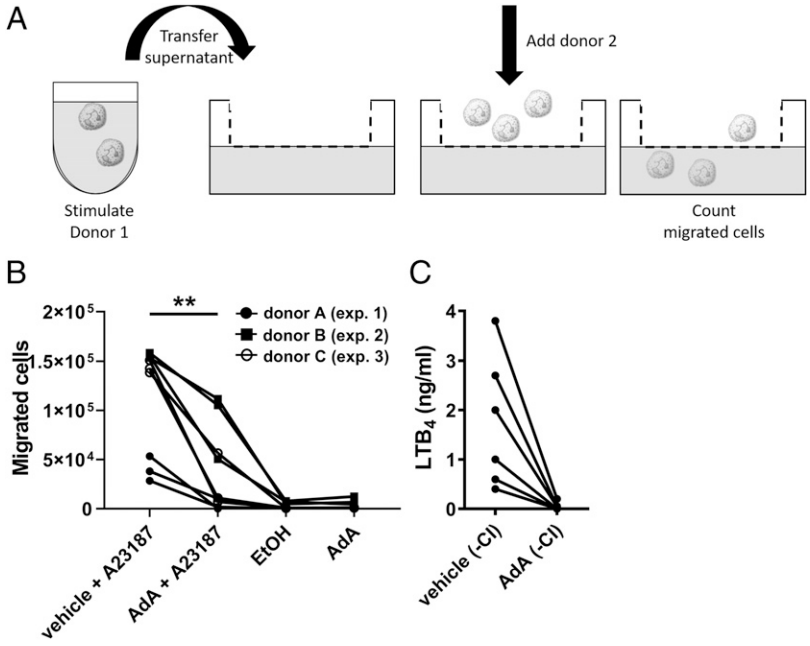

FIGURE 3. Migration toward soluble factors released by neutrophils activated in the presence of AdA is impaired. (**A**) Schematic overview of the chemotaxis experiment. (**B**) Migration of neutrophils toward supernatant of neutrophils treated with AdA or vehicle (1% EtOH) and stimulated with calcium ionophore A23187 or not. Number of migrated neutrophils was determined after 90 min. $n = 3$ donors tested, each with supernatants of three independent donors in three independent experiments. Donors B and C tested with the same set of supernatants. Statistical significance was established using a Wilcoxon signed-rank test. (**C**) Concentrations of LTB_4 in the supernatants were determined by LC-MS/MS and quantified using an external calibration line (ranging from 0 to 5 ng/ml). Controls were performed in triplicates, means of $n = 6$ donors are shown. $^{**}p < 0.01$.

more detail the compartments from which AA is released, using the Lipidyzer platform. We were able to confirm the blunted calcium ionophore A23187–mediated AA release in the presence of AdA using this platform (Fig. 6B). This effect was specific for AA, as AdA had no effect of free LA or DHA levels (Supplemental Fig. 3B, 3C). In contrast to the clear effect of AdA exposure on free AA release, we could not detect any build-up or (re)arrangement of AA in any of the lipid compartments in which we detected AA (Fig. 6C, 6D).

AdA protects from neutrophil-mediated experimental arthritis

Having observed abrogated LTB_4 synthesis, neutrophil migration, and enhanced phagocytosis upon AdA treatment, we investigated the in vivo relevance of these findings. Because our results show inhibited neutrophil attraction by neutrophils exposed to AdA, we investigated the anti-inflammatory and proresolving effects of AdA in the K/BxN serum transfer arthritis model. This model has been shown to be critically dependent on LTB_4 production by neutrophils (35). In line with those results, we observed that AdA limited the severity of arthritis in two independent experiments carried out in two independent facilities (Fig. 7A). In both experiments, we showed a decreased clinical score in AdA-treated mice, as well as a decrease in ankle thickness measured in one of the experiments (Fig. 7A, Supplemental Fig. 4A). Interestingly, the reduced arthritis severity correlated with lower levels of anti-G6PI Abs in the serum of the AdA-treated mice (Fig. 7C, 7D). The lower titers were not due to AdA interfering with the ELISA (Supplemental Fig. 4B).

Discussion

In this study, we investigated the kinetics of both *n*-3 and *n*-6 PUFAs in the context of resolution of inflammation. We demonstrated an accumulation of the *n*-6 PUFA AdA in the resolution phase of the self-resolving peritonitis model. Specifically, in neutrophils, AdA potently inhibited AA release and LTB_4 production, reducing further attraction of neutrophils to the site of inflammation. Furthermore, AdA enhanced phagocytosis and efferocytosis by macrophages in vitro and the clearance of neutrophils in the peritonitis model in vivo. Finally, AdA clearly showed the potential to prevent inflammation in the K/BxN serum transfer model of arthritis. These findings indicate a novel anti-inflammatory/proresolving function for the *n*-6 PUFA AdA. Our data supports the notion that *n*-6 PUFAs are not only proinflammatory but can have potent anti-inflammatory

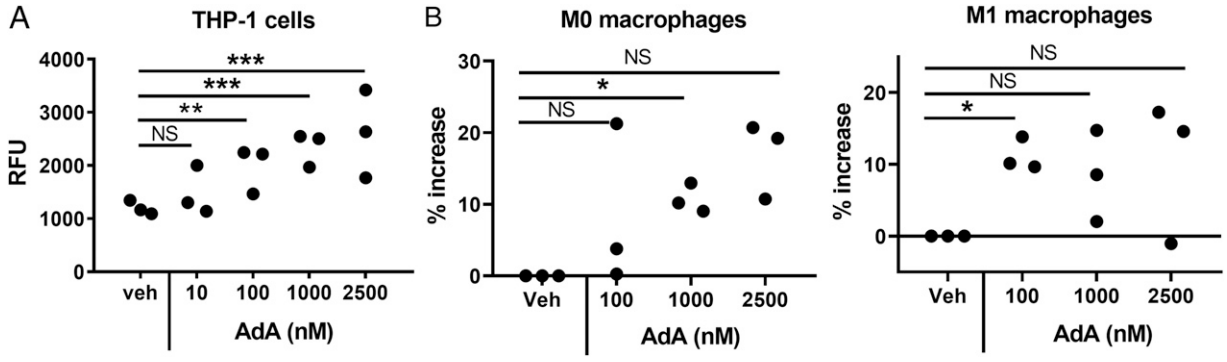

FIGURE 4. AdA enhances phagocytosis. (**A**) Phagocytosis of opsonized fluorescent zymosan particles by THP-1–derived macrophages. Mean values of $n = 3$ donors performed in quadruplicates in three independent experiments. (**B**) Efferocytosis of apoptotic HL-60 cells by M0 and M1 macrophages. $n = 3$ macrophage donors in three independent experiments. Linear-mixed model was performed to show statistical significance. $^{*}p < 0.05$, $^{**}p < 0.01$, $^{***}p < 0.001$. RFU, relative fluorescent unit.

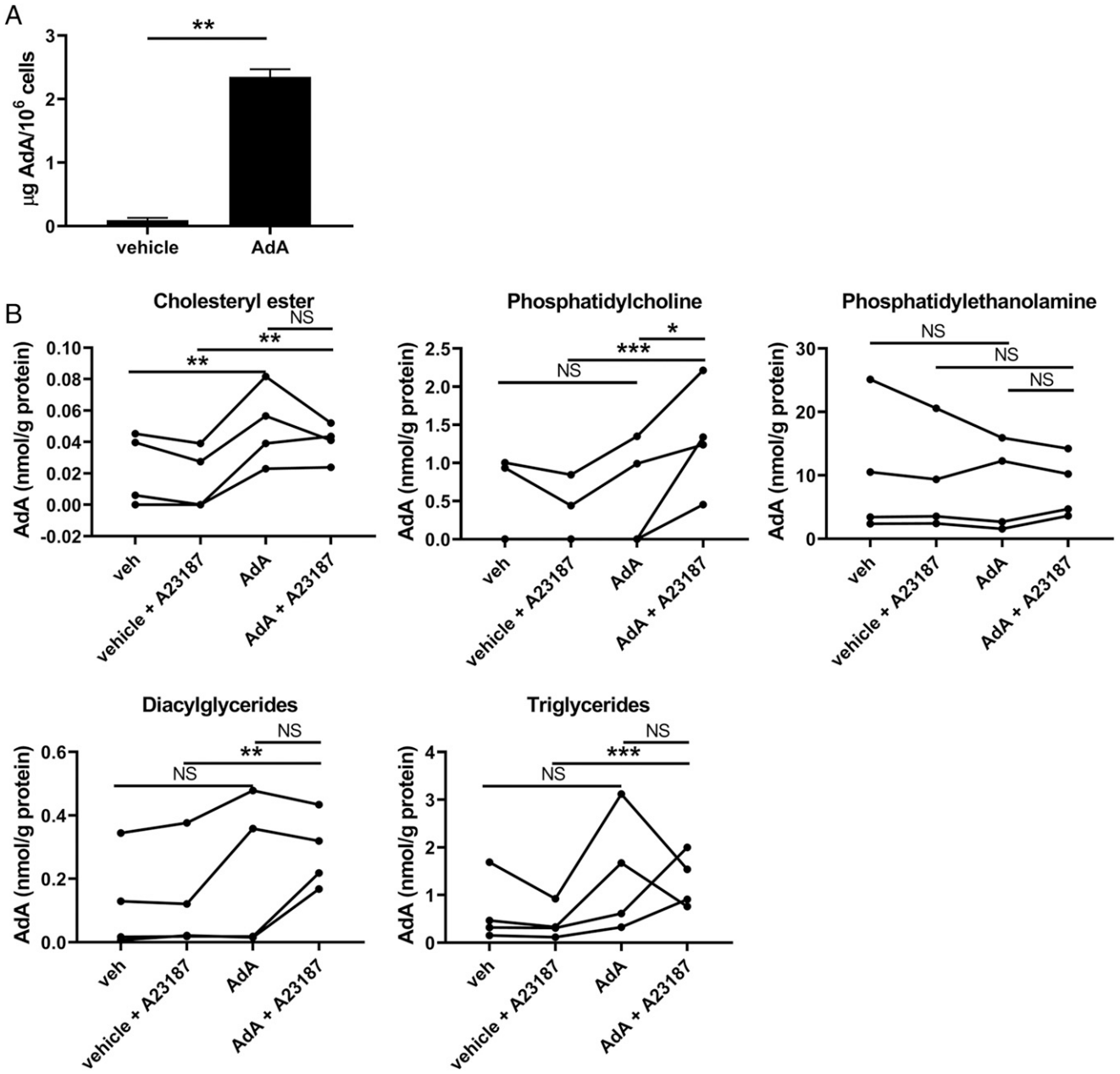

FIGURE 5. AdA incorporates in different fatty acid reservoirs in neutrophils. (**A**) Neutrophils were incubated with AdA or vehicle for 20 min. Total levels of cellular AdA were quantified upon hydrolysis, using GC-MS. Three individual experiments were performed in triplicates; means and SD of $n = 3$ donors are shown. One-way ANOVA was performed. (**B**) Neutrophils were incubated with AdA or vehicle for 10 min and were subsequently stimulated with calcium ionophore A23187 or vehicle for 10 min. Next, cells were subjected to DMS-MS/MS using the Lipidyzer platform and cellular AdA concentrations in various lipid classes were determined. Experiments were performed in triplicates and each line represents a donor ($n = 4$ donors in four independent experiments). Matched two-way ANOVA was performed to compare baseline levels with AdA incubation, to compare the calcium ionophore A23187 stimulated conditions, and to compare the effect of calcium ionophore A23187 stimulation after AdA incubation and to baseline. Values below detection limit were assigned the null value. $*p < 0.05$, $**p < 0.01$, $***p < 0.001$.

functions as well, and our data set the stage to delineate the mechanisms underlying the biological effects of AdA presented in this study.

Effects of AdA on AA were already proposed in 1980 by indicating that AdA modulates the inflammatory effects of AA as AdA limited the fall in blood pressure induced by AA injections in rats (16). A few years later, it was shown that this effect of AdA is due to the inhibition of PG I_2 formation by competing with AA for cyclooxygenase enzymes as well as by reducing the AA content of phosphatidylinositol structures in human endothelial cells (17, 18). In this study, we were unable to show build-up or (re)arrangement of AA levels in various lipid compartments. However, this is probably due to the relatively small amount of AA that is prevented from becoming free fatty acid compared with the total amount of AA in the cell. Alternatively, AA might be released from lipid species we were technically not able to measure, as for example phosphatidylinositol lipids. Because AdA did not affect lipase activity, we hypothesize that AdA might cause a strong activation of acyltransferases, for example the diglycerideacyltransferases, could compensate the $cPLA_2$ effects upon calcium ionophore A23187 activation and reverse the balance from free AA to esterified AA.

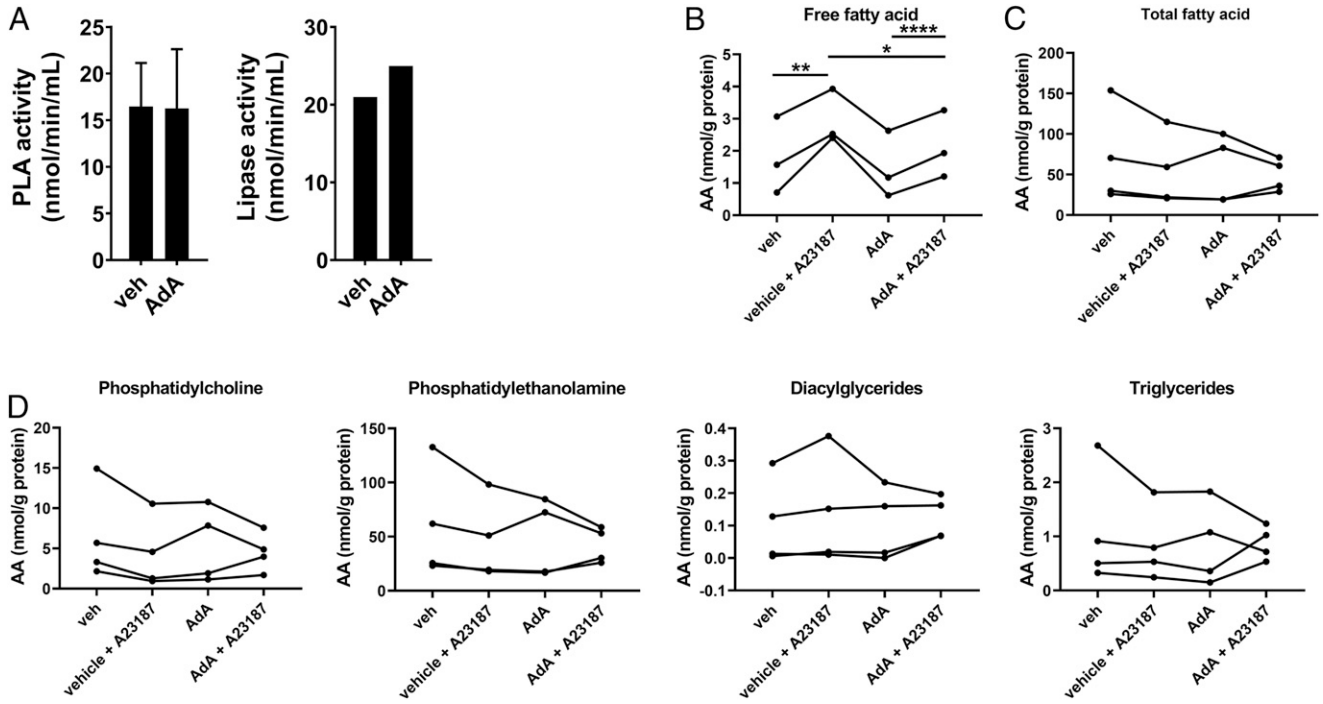

FIGURE 6. AA concentrations in higher-order lipid compartments (**A**) Neutrophils pretreated with AdA or vehicle for 10 min were stimulated with calcium ionophore A23187 for 2 (phospholipase [PLA]) or 10 (lipase) minutes. Enzyme activity was determined using activity assays. Means are shown for both assays and SD are shown for PLA activity. $n = 3$ (PLA) and $n = 2$ (lipase), all performed in individual experiments. (**B**–**D**) Neutrophils were incubated with AdA or vehicle for 10 min. Subsequently, they were stimulated with calcium ionophore A23187 or vehicle for 10 min. Next, the cells were subjected to DMS-MS/MS using the Lipidyzer platform. Cellular AA levels, free (B), total (C), and within the PC, PE, DAG, and TAG classes (D) are shown. Experiments were performed in triplicates, and values below detection limit were assigned the null value. Each line represents one donor ($n = 4$ in four independent experiments). Matched two-way ANOVA was performed comparing the same conditions as for Fig. 5.*$p < 0.05$, **$p < 0.01$, ****$p < 0.0001$.

The effect of AdA seems to be specific for AA, as we did not observe this with another *n*-6 PUFA, LA, nor with the *n*-3 PUFAs DHA and EPA.

The finding that AdA accumulated specifically inside the cells during the resolution phase strongly points to the activation of a cell-intrinsic mechanism to initiate the resolution phase. The source of AdA might be AA itself because AA can be converted into AdA by elongases as previously shown in RAW 264.7 macrophages (36). This could be a mechanism by which the cells remove the no-longer-needed substrate AA.

As we observed potent effects of AdA on LTB_4 production in neutrophils, we have investigated the effect of AdA in an in vivo inflammatory model dependent on LTB_4 production by neutrophils (35). In the K/BxN serum–transferred arthritis model, we expected that AdA would impair the capacity of neutrophils to further amplify the inflammation through the production of LTB_4. Indeed, we observed a potent anti-inflammatory effect of AdA. Unexpectedly, we observed a decrease in the arthritogenic anti-G6PI Abs in the AdA-treated mice, in association with the lower clinical arthritis score. Because all mice received the same amount of serum containing the Abs, we hypothesize that these Abs might be cleared from the circulation faster than in the untreated mice. Indeed, we show that plasma titers of treated mice are already lower than those of untreated mice at day 10 of the experiment. These results are in line with the enhanced ability of AdA-exposed macrophages to phagocytose, possibly allowing the enhanced clearance of arthritogenic immune complexes by these macrophages. Indeed, it is known that anti-G6PI Abs form immune complexes (37, 38). We therefore propose that, in addition to inhibiting neutrophil-derived LTB_4 production, AdA might also enhance the macrophage-mediated clearance of anti-G6PI Abs in this model.

The increase in AdA levels and the disappearance of LTB_4 from the peritoneal cavity at the initiation of the resolution phase is consistent with our finding that neutrophils exposed to AdA inhibit LTB_4 production. However, AA and AA metabolites such as PGE_2 and TXB_2 still increase while AdA levels are also increased. Because there are predominantly macrophages in the peritoneum at this timepoint, the increase of AA and AA metabolites point toward a different proresolving activity than what we show in neutrophils. For example, it was shown that macrophage populations sustain PGE_2 production during the late resolution phases in murine peritonitis to prevent autoimmune reactions (39).

Consistent with the data presented in this study, the same effect on LTB_4 production in neutrophils has been described by others after dietary *n*-3 supplementation with EPA and DHA (40, 41). However, this is the first time, to our knowledge, that the effect on LTB_4 production has been described for an *n*-6 PUFA, and the effect of AdA has never been tested in clinical trials. Although it is likely that the results presented in this study are due to the effects of AdA, we have not investigated whether AdA is enzymatically or nonenzymatically converted to any downstream products such as the 15-LOX metabolite 17-HDoTE (42).

Our data emphasize that *n*-6 fatty acids should not be categorized as merely proinflammatory as they can have potent anti-inflammatory effects as well. Importantly, they highlight a previously unappreciated anti-inflammatory and proresolving effect of AdA, offering an emerging therapeutic candidate in inflammatory disease such as atherosclerosis, autoimmune diseases, asthma, and cancer.

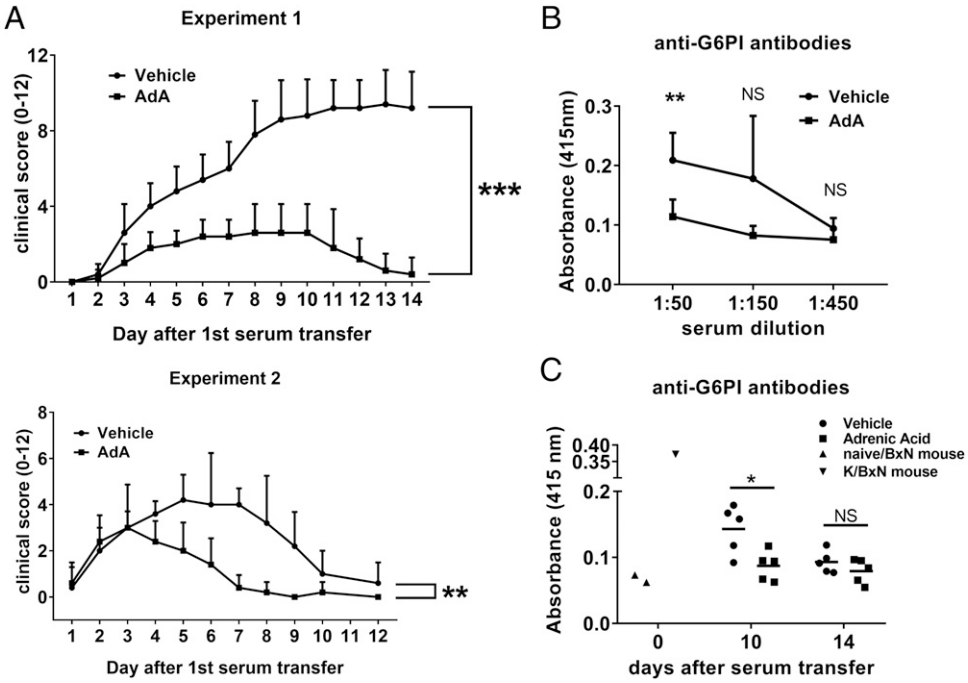

FIGURE 7. AdA reduces severity of neutrophil-mediated experimental arthritis. (**A**) Clinical arthritis scores are shown for two independent experiments executed independently in two different laboratories. Mice were administered AdA from day –3 till the end of the experiment. Mean and SD are shown ($n = 5$ mice per group per experiment). Statistical significance was established using a repeated measures ANOVA as a mixed model. (**B**) Serum anti-G6PI Abs of day 14 measured by ELISA in mice from experiment 1. Mean and SD are shown. (**C**) Anti-G6PI Abs over time of experiment 2 together with controls. Plasma was diluted 1:100. Each dot represents a mouse, and the mean of duplicates is shown. Statistical significance in (B) and (C) was established using Student t tests. $*p < 0.05$, $**p < 0.01$, $***p < 0.001$.

Disclosures

The authors have no financial conflicts of interest.

References

1. Serhan, C. N. 2014. Pro-resolving lipid mediators are leads for resolution physiology. *Nature* 510: 92–101.
2. Harris, W. S. 2018. The Omega-6:Omega-3 ratio: a critical appraisal and possible successor. *Prostaglandins Leukot. Essent. Fatty Acids* 132: 34–40.
3. Serhan, C. N., S. Hong, K. Gronert, S. P. Colgan, P. R. Devchand, G. Mirick, and R.-L. Moussignac. 2002. Resolvins: a family of bioactive products of omega-3 fatty acid transformation circuits initiated by aspirin treatment that counter proinflammation signals. *J. Exp. Med.* 196: 1025–1037.
4. Spite, M., L. V. Norling, L. Summers, R. Yang, D. Cooper, N. A. Petasis, R. J. Flower, M. Perretti, and C. N. Serhan. 2009. Resolvin D2 is a potent regulator of leukocytes and controls microbial sepsis. *Nature* 461: 1287–1291.
5. Hong, S., K. Gronert, P. R. Devchand, R.-L. Moussignac, and C. N. Serhan. 2003. Novel docosatrienes and 17S-resolvins generated from docosahexaenoic acid in murine brain, human blood, and glial cells. Autacoids in anti-inflammation. *J. Biol. Chem.* 278: 14677–14687.
6. Kumar, N., G. Gupta, K. Anilkumar, N. Fatima, R. Karnati, G. V. Reddy, P. V. Giri, and P. Reddanna. 2016. 15-Lipoxygenase metabolites of α-linolenic acid, [13-(S)-HPOTrE and 13-(S)-HOTrE], mediate anti-inflammatory effects by inactivating NLRP3 inflammasome. *Sci. Rep.* 6: 31649.
7. Calder, P. C. 2010. Omega-3 fatty acids and inflammatory processes. *Nutrients* 2: 355–374.
8. Norris, P. C., and E. A. Dennis. 2012. Omega-3 fatty acids cause dramatic changes in TLR4 and purinergic eicosanoid signaling. *Proc. Natl. Acad. Sci. USA* 109: 8517–8522.
9. Oh, D. Y., S. Talukdar, E. J. Bae, T. Imamura, H. Morinaga, W. Fan, P. Li, W. J. Lu, S. M. Watkins, and J. M. Olefsky. 2010. GPR120 is an omega-3 fatty acid receptor mediating potent anti-inflammatory and insulin-sensitizing effects. *Cell* 142: 687–698.
10. Serhan, C. N., M. Hamberg, and B. Samuelsson. 1984. Lipoxins: novel series of biologically active compounds formed from arachidonic acid in human leukocytes. *Proc. Natl. Acad. Sci. USA* 81: 5335–5339.
11. Gilroy, D. W., M. L. Edin, R. P. H. De Maeyer, J. Bystrom, J. Newson, F. B. Lih, M. Stables, D. C. Zeldin, and D. Bishop-Bailey. 2016. CYP450-derived oxylipins mediate inflammatory resolution. *Proc. Natl. Acad. Sci. USA* 113: E3240–E3249.
12. Ricciotti, E., and G. A. FitzGerald. 2011. Prostaglandins and inflammation. *Arterioscler. Thromb. Vasc. Biol.* 31: 986–1000.
13. Pullman-Mooar, S., M. Laposata, D. Lem, R. T. Holman, L. J. Leventhal, D. DeMarco, and R. B. Zurier. 1990. Alteration of the cellular fatty acid profile and the production of eicosanoids in human monocytes by gamma-linolenic acid. *Arthritis Rheum.* 33: 1526–1533.
14. Iversen, L., K. Fogh, G. Bojesen, and K. Kragballe. 1991. Linoleic acid and dihomogammalinolenic acid inhibit leukotriene B4 formation and stimulate the formation of their 15-lipoxygenase products by human neutrophils in vitro. Evidence of formation of antiinflammatory compounds. *Agents Actions* 33: 286–291.
15. Iversen, L., K. Fogh, and K. Kragballe. 1992. Effect of dihomogammalinolenic acid and its 15-lipoxygenase metabolite on eicosanoid metabolism by human mononuclear leukocytes in vitro: selective inhibition of the 5-lipoxygenase pathway. *Arch. Dermatol. Res.* 284: 222–226.
16. Cagen, L. M., and P. G. Baer. 1980. Adrenic acid inhibits prostaglandin syntheses. *Life Sci.* 26: 765–770.
17. Mann, C. J., T. L. Kaduce, P. H. Figard, and A. A. Spector. 1986. Docosatetraenoic acid in endothelial cells: formation, retroconversion to arachidonic acid, and effect on prostacyclin production. *Arch. Biochem. Biophys.* 244: 813–823.
18. Campbell, W. B., J. R. Falck, J. R. Okita, A. R. Johnson, and K. S. Callahan. 1985. Synthesis of dihomoprostaglandins from adrenic acid (7,10,13,16-docosatetraenoic acid) by human endothelial cells. *Biochim. Biophys. Acta* 837: 67–76.
19. Reisman, J., H. M. Schachter, R. E. Dales, K. Tran, K. Kourad, D. Barnes, M. Sampson, A. Morrison, I. Gaboury, and J. Blackman. 2006. Treating asthma with omega-3 fatty acids: where is the evidence? A systematic review. *BMC Complement. Altern. Med.* 6: 26.
20. Miles, E. A., and P. C. Calder. 2012. Influence of marine n-3 polyunsaturated fatty acids on immune function and a systematic review of their effects on clinical outcomes in rheumatoid arthritis. *Br. J. Nutr.* 107(Suppl. 2): S171–S184.
21. Senftleber, N. K., S. M. Nielsen, J. R. Andersen, H. Bliddal, S. Tarp, L. Lauritzen, D. E. Furst, M. E. Suarez-Almazor, A. Lyddiatt, and R. Christensen. 2017. Marine oil supplements for arthritis pain: a systematic review and meta-analysis of randomized trials. *Nutrients* 9: 42.
22. Balk, E. M., G. P. Adams, V. Langberg, C. Halladay, M. Chung, L. Lin, S. Robertson, A. Yip, D. Steele, B. T. Smith, et al. 2016. Omega-3 fatty acids and cardiovascular disease: an updated systematic review. Rockville, MD: Agency for Healthcare Research and Quality. Evidence Report/Technology Assessment, No. 223. Available at: https://effectivehealthcare.ahrq.gov/sites/default/files/pdf/fatty-acids-cardiovascular-disease_research.pdf.
23. Bowen, K. J., W. S. Harris, and P. M. Kris-Etherton. 2016. Omega-3 fatty acids and cardiovascular disease: are there benefits? *Curr. Treat. Options Cardiovasc. Med.* 18: 69.
24. Farvid, M. S., M. Ding, A. Pan, Q. Sun, S. E. Chiuve, L. M. Steffen, W. C. Willett, and F. B. Hu. 2014. Dietary linoleic acid and risk of coronary heart disease: a systematic review and meta-analysis of prospective cohort studies. *Circulation* 130: 1568–1578.

25. Wu, J. H. Y., M. Marklund, F. Imamura, N. Tintle, A. V. Ardisson Korat, J. de Goede, X. Zhou, W. S. Yang, M. C. de Oliveira Otto, J. Kröger, et al; Cohorts for Heart and Aging Research in Genomic Epidemiology (CHARGE) Fatty Acids and Outcomes Research Consortium (FORCE). 2017. Omega-6 fatty acid biomarkers and incident type 2 diabetes: pooled analysis of individual-level data for 39 740 adults from 20 prospective cohort studies. *Lancet Diabetes Endocrinol.* 5: 965–974.
26. Giera, M., A. Ioan-Facsinay, R. Toes, F. Gao, J. Dalli, A. M. Deelder, C. N. Serhan, and O. A. Mayboroda. 2012. Lipid and lipid mediator profiling of human synovial fluid in rheumatoid arthritis patients by means of LC-MS/MS. *Biochim. Biophys. Acta* 1821: 1415–1424.
27. Monach, P., K. Hattori, H. Huang, E. Hyatt, J. Morse, L. Nguyen, A. Ortiz-Lopez, H.-J. Wu, D. Mathis, and C. Benoist. 2007. The K/BxN mouse model of inflammatory arthritis: theory and practice. *Methods Mol. Med.* 136: 269–282.
28. Nguyen, L. T., J. Jacobs, D. Mathis, and C. Benoist. 2007. Where FoxP3-dependent regulatory T cells impinge on the development of inflammatory arthritis. *Arthritis Rheum.* 56: 509–520.
29. Bannenberg, G. L., N. Chiang, A. Ariel, M. Arita, E. Tjonahen, K. H. Gotlinger, S. Hong, and C. N. Serhan. 2005. Molecular circuits of resolution: formation and actions of resolvins and protectins. *J. Immunol.* 174: 4345–4355.
30. Fredman, G., Y. Li, J. Dalli, N. Chiang, and C. N. Serhan. 2012. Self-limited versus delayed resolution of acute inflammation: temporal regulation of pro-resolving mediators and microRNA. *Sci. Rep.* 2: 639.
31. Bystrom, J., I. Evans, J. Newson, M. Stables, I. Toor, N. van Rooijen, M. Crawford, P. Colville-Nash, S. Farrow, and D. W. Gilroy. 2008. Resolution-phase macrophages possess a unique inflammatory phenotype that is controlled by cAMP. *Blood* 112: 4117–4127.
32. Prame Kumar, K., A. J. Nicholls, and C. H. Y. Wong. 2018. Partners in crime: neutrophils and monocytes/macrophages in inflammation and disease. *Cell Tissue Res.* 371: 551–565.
33. Marshall, J., E. Krump, T. Lindsay, G. Downey, D. A. Ford, P. Zhu, P. Walker, and B. Rubin. 2000. Involvement of cytosolic phospholipase A2 and secretory phospholipase A2 in arachidonic acid release from human neutrophils. *J. Immunol.* 164: 2084–2091.
34. Schlager, S., M. Goeritzer, K. Jandl, R. Frei, N. Vujic, D. Kolb, H. Strohmaier, J. Dorow, T. O. Eichmann, A. Rosenberger, et al. 2015. Adipose triglyceride lipase acts on neutrophil lipid droplets to regulate substrate availability for lipid mediator synthesis. *J. Leukoc. Biol.* 98: 837–850.
35. Chen, M., B. K. Lam, Y. Kanaoka, P. A. Nigrovic, L. P. Audoly, K. F. Austen, and D. M. Lee. 2006. Neutrophil-derived leukotriene B_4 is required for inflammatory arthritis. *J. Exp. Med.* 203: 837–842.
36. Guijas, C., A. M. Astudillo, L. Gil-de-Gómez, J. M. Rubio, M. A. Balboa, and J. Balsinde. 2012. Phospholipid sources for adrenic acid mobilization in RAW 264.7 macrophages. Comparison with arachidonic acid. *Biochim. Biophys. Acta* 1821: 1386–1393.
37. Binstadt, B. A., P. R. Patel, H. Alencar, P. A. Nigrovic, D. M. Lee, U. Mahmood, R. Weissleder, D. Mathis, and C. Benoist. 2006. Particularities of the vasculature can promote the organ specificity of autoimmune attack. *Nat. Immunol.* 7: 284–292.
38. Maccioni, M., G. Zeder-Lutz, H. Huang, C. Ebel, P. Gerber, J. Hergueux, P. Marchal, V. Duchatelle, C. Degott, M. van Regenmortel, et al. 2002. Arthritogenic monoclonal antibodies from K/BxN mice. *J. Exp. Med.* 195: 1071–1077.
39. Newson, J., M. P. Motwani, A. C. Kendall, A. Nicolaou, G. G. Muccioli, M. Alhouayek, M. Bennett, R. Van De Merwe, S. James, R. P. H. De Maeyer, and D. W. Gilroy. 2017. Inflammatory resolution triggers a prolonged phase of immune suppression through COX-1/mPGES-1-derived prostaglandin E_2. *Cell Rep.* 20: 3162–3175.
40. Sperling, R. I., A. I. Benincaso, C. T. Knoell, J. K. Larkin, K. F. Austen, and D. R. Robinson. 1993. Dietary omega-3 polyunsaturated fatty acids inhibit phosphoinositide formation and chemotaxis in neutrophils. *J. Clin. Invest.* 91: 651–660.
41. Lee, T. H., R. L. Hoover, J. D. Williams, R. I. Sperling, J. Ravalese, III, B. W. Spur, D. R. Robinson, E. J. Corey, R. A. Lewis, and K. F. Austen. 1985. Effect of dietary enrichment with eicosapentaenoic and docosahexaenoic acids on in vitro neutrophil and monocyte leukotriene generation and neutrophil function. *N. Engl. J. Med.* 312: 1217–1224.
42. Jónasdóttir, H. S., H. Brouwers, J. C. Kwekkeboom, H. M. J. van der Linden, T. Huizinga, M. Kloppenburg, R. E. M. Toes, M. Giera, and A. Ioan-Facsinay. 2017. Targeted lipidomics reveals activation of resolution pathways in knee osteoarthritis in humans. *Osteoarthritis Cartilage* 25: 1150–1160.